


Article

The H₂O Effect on Cu Speciation in Cu-CHA-Catalysts for NH₃-SCR Probed by NH₃ Titration

Roberta Villamaina¹, Federica Gramigni¹, Umberto Iacobone¹, Shaojun Liu¹ , Isabella Nova¹, Enrico Tronconi^{1,*}, Maria Pia Ruggeri², Jillian Collier², Andrew P. E. York² and David Thompsett²

¹ Laboratory of Catalysis and Catalytic Processes, Dipartimento di Energia, Politecnico di Milano, via La Masa 34, 20156 Milano, Italy; roberta.villamaina@polimi.it (R.V.); federica.gramigni@polimi.it (F.G.); umberto.iacobone@polimi.it (U.I.); shaojun.liu@polimi.it (S.L.); isabella.nova@polimi.it (I.N.)

² Johnson Matthey Technology Centre, Blounts Court Road, Sonning Common, Reading RG4 9NH, UK; MariaPia.Ruggeri@matthey.com (M.P.R.); jillian.collier@matthey.com (J.C.); andrew.york@matthey.com (A.P.E.Y.); david.thompsett@matthey.com (D.T.)

* Correspondence: enrico.tronconi@polimi.it

Abstract: The present work is focused on the effect of water on NH₃ adsorption over Cu-CHA SCR catalysts. For this purpose, samples characterized by different SAR (SiO₂/Al₂O₃) ratios and Cu loadings were studied under both dry and wet conditions. H₂O adversely affects NH₃ adsorption on Lewis acid sites (Cu ions) over all the tested catalysts, as indicated by the decreased NH₃ desorption at low temperature during TPD. Interestingly, the NH₃/Cu ratio, herein regarded as an index for the speciation of Cu cations, fell in the range of 3–4 (in the presence of gaseous NH₃) or 1–2 (no gaseous NH₃) in dry conditions, in line with the formation of different NH₃-solvated Cu species (e.g., [Cu^{II}(NH₃)₄]²⁺ and [Cu^{II}(OH)(NH₃)₃]⁺ with gaseous NH₃, [Z₂Cu^{II}(NH₃)₂]²⁺ and [ZCu^{II}(OH)(NH₃)]⁺ without gaseous NH₃). When H₂O was fed to the system, on the contrary, the NH₃/Cu ratio was always close to 3 (or 1), while the Brønsted acidity was slightly increased. These results are consistent both with competition between H₂O and NH₃ for adsorption on Lewis sites and with the hydrolysis of a fraction of Z₂Cu^{II} species into ZCu^{II}OH.

Keywords: Cu-CHA; NH₃-SCR; Si/Al ratio; Cu loading; H₂O effect; Cu speciation



Citation: Villamaina, R.; Gramigni, F.; Iacobone, U.; Liu, S.; Nova, I.; Tronconi, E.; Ruggeri, M.P.; Collier, J.; York, A.P.E.; Thompsett, D. The H₂O Effect on Cu Speciation in Cu-CHA-Catalysts for NH₃-SCR Probed by NH₃ Titration. *Catalysts* **2021**, *11*, 759. <https://doi.org/10.3390/catal11070759>

Academic Editors: Maria Casapu and Dmitry E. Doronkin

Received: 28 May 2021
Accepted: 14 June 2021
Published: 23 June 2021

Publisher's Note: MDPI stays neutral with regard to jurisdictional claims in published maps and institutional affiliations.

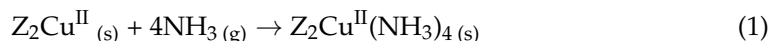


Copyright: © 2021 by the authors. Licensee MDPI, Basel, Switzerland. This article is an open access article distributed under the terms and conditions of the Creative Commons Attribution (CC BY) license (<https://creativecommons.org/licenses/by/4.0/>).

1. Introduction

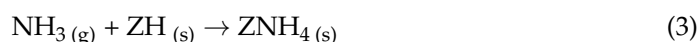
NH₃/urea SCR is recognized worldwide as an effective technology in controlling automotive emissions to meet increasingly stricter NO_x emission regulations [1,2]. Amongst state-of-the-art metal-promoted zeolite catalysts used in this process, Cu-exchanged chabazite (Cu-CHA) shows excellent activity and extraordinary hydrothermal stability over a broad temperature range under SCR conditions, triggering intensive research on the relationship between its unique structure and its DeNO_x performance [3–11]. In this regard, the SiO₂/Al₂O₃ ratio (SAR) and the Cu loading content are important structure indexes, which could affect the nature of Cu cations existing in the catalyst framework and, based on their nature, location and redox properties, further impact the SCR activity [3–9]. Two Cu species are recognized to be present in the Cu-CHA catalyst: Z₂Cu^{II} (doubly coordinated to the framework) and ZCu^{II}OH (balanced by one framework negative charge), whose relative ratio can be predicted based on Si/Al and Cu/Al ratios [5,6,11]. The proportion of such Cu species could also be affected by several factors, for example, hydrothermal aging [4,6,12] or hydrated/dehydrated conditions [5,6]. It was also proposed, based on DFT calculations, DRIFTS, XAS and NH₃-TPD tests [4,5,8,13], that these two species are able to coordinate a different number of NH₃ molecules, thus influencing, in turn, the NH₃ storage capacity, a relevant parameter for the SCR process. In line with Paolucci et al. [5], our recent paper concluded that upon full catalyst saturation, the Z₂Cu^{II} species could coordinate up to four NH₃ molecules, while the hydroxylated Cu^{II} site could bind only three molecules [8]. The

NH₃ adsorption chemistry on the Lewis acid sites can be summarized by the following reactions [13]:



When Cu-CHA catalysts were not fully saturated and Cu ions were not able to detach from the zeolite framework, however, we observed a stoichiometry different from reaction (1) and (2) for the two copper species: Z₂Cu^{II} ions adsorb two NH₃ molecules while only one NH₃ is bound to ZCu^{II}OH, in agreement with Luo et al. [4].

NH₃ can also be adsorbed on the Brønsted acid sites typical of the zeolite framework, according to the adsorption chemistry reported below [12]:



Herein, we carried out NH₃ adsorption + TPD tests under both dry and wet conditions over several Cu-CHA samples with different SARs and Cu loadings, which therefore contain distinct fractions of the two Cu species populations and different Brønsted sites [5,8]. The aim of the present investigation is to verify if H₂O affects the Lewis and Brønsted acidity in chabazite-based materials and the possibility to use NH₃-TPD as a probe technique for Cu speciation. In the literature, this method was implemented to characterize Cu-CHA catalysts in dry environments only in [8] or in the presence of water only in [4,12]. On the contrary, to assess the role of H₂O in NH₃ adsorption, we compared the performance of different samples under both wet and dry conditions.

2. Results and Discussion

An example of an NH₃ adsorption/desorption run is provided in Figure 1A, depicting the three stages of the test, namely isothermal adsorption, isothermal desorption, and TPD. The run was performed after having pre-oxidized the sample at 550 °C. The aim was not only to evaluate the NH₃ storage capacity, but more specifically to identify the different sites present in the catalyst [8].

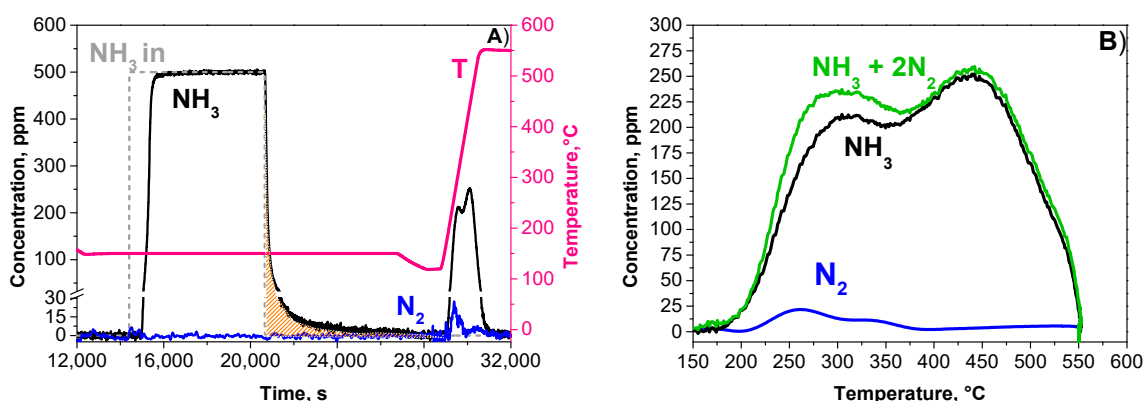


Figure 1. (A) NH₃ adsorption + TPD test over 1.7Cu-CHA 25 catalyst. GHSV = 266,250 cm³/(g_{cat}*h) (STP). Pre-oxidized catalysts. NH₃ = 500 ppm, TPD heating rate = 15 °C/min, He. (B) TPD plot.

For this purpose, we analyze the TPD phase. As shown in Figure 1A, the temperature ramp featured a release of NH₃ together with a small N₂ peak (about 25 ppm). The integral of the N₂ released (i.e., ≈0.68 μmol) is in line with the full reduction in Cu^{II} ions (i.e., 4.3 μmol of Cu loaded) by adsorbed NH₃ according to the following stoichiometries [13,14]:

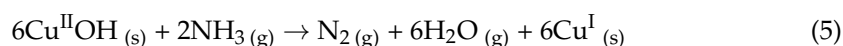
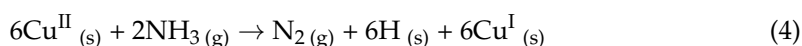


Figure 1B displays the NH_3 and N_2 traces during the TPD, whereas the corresponding integral balances are reported in Table 1. The N balance error improves significantly if the production of nitrogen is taken into account. In line with this result, Borfecchia et al. showed by means of XAS spectroscopy and UV-vis-NIR experiments that at the end of the TPD, after NH_3 adsorption, the Cu sites in their Cu-CHA catalysts were almost completely reduced [13].

Table 1. Integral balances for the NH_3 adsorption + TPD test over 1.7Cu-CHA25 shown in Figure 1.

1.7Cu-CHA25	
Cu_{tot} (ICP) (μmol)	4.3
NH_3 adsorbed (μmol)	23.4
NH_3 physisorbed (μmol)	8.0
NH_3 chemisorbed (μmol)	14.1
N_2 produced (μmol)	0.7
N balance error w/o N_2 (%)	5.6
N balance error with N_2 (%)	0.1

In line with the literature, the TPD curve in Figure 1B showed two distinct NH_3 release peaks, ascribed to energetically different populations of acidic sites [4,8,15] (Figure 2). The physical nature of the different sites was estimated via Gaussian deconvolution of the NH_3 -TPD trace, to which the contribution of N_2 according to the reactions discussed above (4) and (5) was added (green line in Figures 1B and 2). The N_2 trace was not measured in our previous investigation [8]; however, it is important to include this contribution to quantify more accurately the various Cu sites taking part in the SCR chemistry.

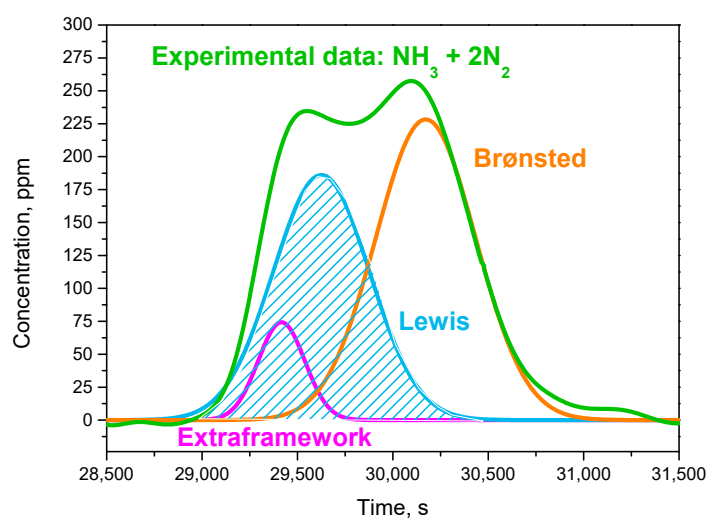


Figure 2. Deconvolution of the NH_3 -TPD profile over 1.7Cu-CHA 25 catalyst in Figure 1B.

As established in several works within the literature [4,8,12,16], the first peak in Figure 1B is related to the NH_3 adsorbed onto both Cu species and a small amount of Al extra-framework (quantified in [8] and reported in Table S1), while the second one is attributed to NH_3 desorption from Brønsted sites associated with the bare zeolite framework. It is notable that the nitrogen production in Figure 1A was well aligned with the low temperature peak of the NH_3 -TPD curve, implying that mostly Lewis NH_3 is responsible for the reduction in Cu^{II} cations into Cu^{I} according to (4) and (5).

2.1. H_2O Effect with Changes in Cu Loading

Figure 3 shows the Cu loading effect on the NH_3 -TPD data collected over each catalyst under both dry and wet conditions.

Figure 3A refers to the simplest case, i.e., the TPD profiles over the unpromoted chabazite catalyst with SAR 25. The curves obtained in the presence and absence of H₂O are almost overlapped, showing a single desorption peak centered at about 440 °C with a similar intensity in both tests. This peak corresponds to the desorption of NH₃ stored onto the Brønsted acid sites of the zeolite [11,17–19]. The small shoulder visible at 250 °C under dry conditions (black line) is linked to the extra-framework aluminum species, which confers a slight Lewis acidity to the catalyst [6,17–21]. This peak disappeared under wet conditions, in accordance with findings in the literature [6,20,21].

Interestingly, H₂O significantly affects the weakly bound NH₃, since H₂O molecules are stored preferentially on Lewis acid sites. A clear confirmation of this behavior was obtained comparing the NH₃ desorption profiles of the copper-exchanged samples under dry and wet conditions. Figure 3B–D show the TPD results for the zeolite catalysts with the same SAR (25) and loaded with 0.7, 1.7 and 2.1% *w/w* copper, respectively. The presence of H₂O considerably lowered the NH₃ storage capacity of all catalysts, affecting mostly the low-T peak, associated predominantly with Cu ions. The high-temperature Brønsted NH₃ peak was less affected by H₂O. The negative effect of H₂O on the NH₃ storage capacity of Lewis sites was confirmed by the faster dynamics during the catalyst saturation in the isothermal adsorption phase, when the samples were previously treated with H₂O (not shown): indeed, the dead time recorded during this phase was reduced from 530–860 s under dry conditions to 380–595 s under wet conditions. In addition, the integral of the TPD curves (NH₃ + 2N₂) was lower in the presence of H₂O even considering the negligible contribution of the extra-framework Al sites (Tables S1 and S2).

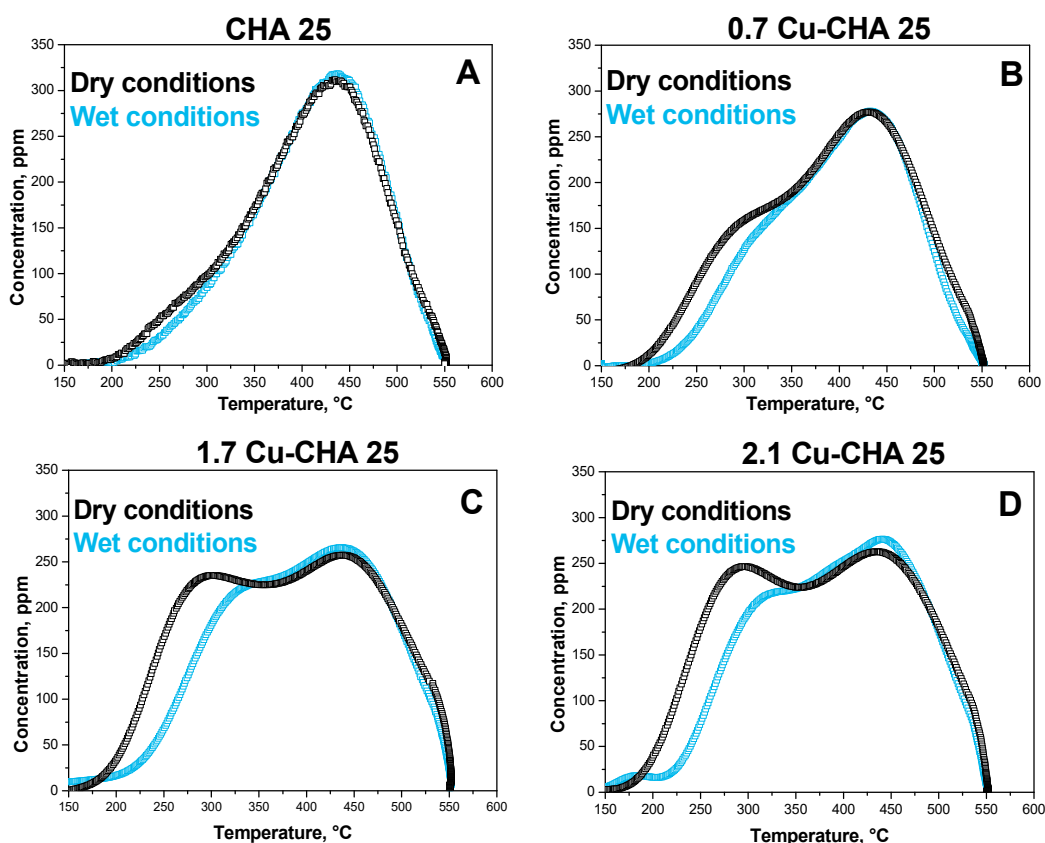


Figure 3. Comparison between dry and wet NH₃-TPD (NH₃ + 2N₂) after adsorption at 150 °C on Cu-CHA catalysts with SAR = 25 and different Cu loadings: (A) 0% *w/w*; (B) 0.7% *w/w*; (C) 1.7% *w/w*; (D) 2.1% *w/w*. NH₃ = 500 ppm, H₂O = 0–5% *v/v*; heating rate = 15 °C/min, He. GHSV = 266,250 cm³/(g_{cat}*h) (STP). Pre-oxidized catalysts.

2.2. Water Effect with Changes in SAR

Results were also collected over Cu-CHA catalysts with fixed Cu loading (1.7% *w/w*) and different SARs (10, 13, 22, 25): the corresponding TPD curves are shown in Figure 4. Under dry conditions, the differences in the relative intensities of the low and high temperature peaks indicate that on increasing the SAR, the overall stability of the adsorbed NH₃ molecules decreased [8]. In fact, in line with our previous studies, intensities of the low-T peaks were lower than those of the high-T peaks for high SARs (22, 25), and the opposite trend was seen at low SARs (10, 13), where the intensities of the low-T peaks were higher [8]. In all cases, the overall amount of chemisorbed NH₃ calculated from the integration of the TPD curves was found fairly constant upon changing the SAR, in the range of 950–1120 μmol/g.

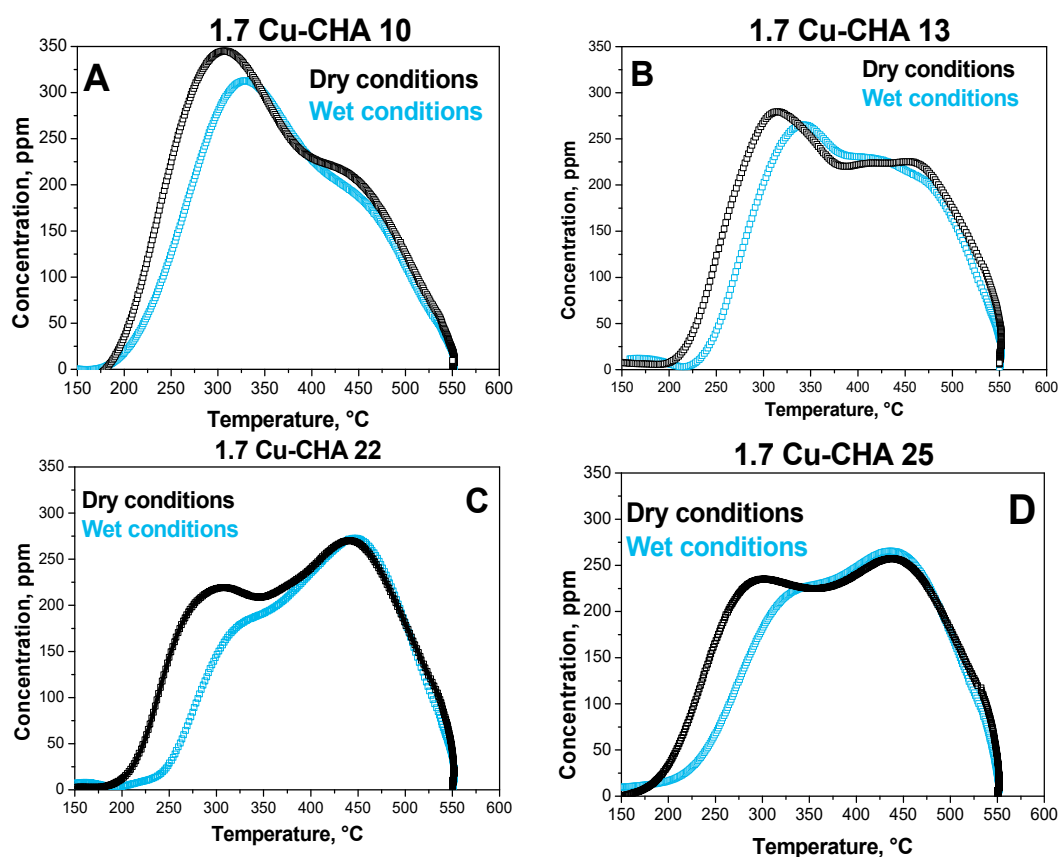


Figure 4. Comparison between dry and wet NH₃-TPD (NH₃ + 2N₂) after adsorption at 150 °C on Cu-CHA catalysts with Cu loading = 1.7% *w/w* and different SAR: (A) 10; (B) 13; (C) 22; (D) 25. NH₃ = 500 ppm, H₂O = 0–5% *v/v*; heating rate = 15 °C/min, He. GHSV = 266,250 cm³/(g_{cat}*h) (STP). Pre-oxidized catalysts.

A similar effect was observed in presence of H₂O (light-blue lines). Comparing the TPD under wet and dry conditions, it is apparent that H₂O reduced ammonia storage (Figure 4). Similarly to the data presented in the previous section, the low-temperature desorption feature diminished as a result of H₂O addition. Furthermore, the overall chemisorbed NH₃ decreased to 830–880 μmol/g for all the catalysts. Accordingly, the deadtime recorded during the adsorption phase was affected by the presence of water (not shown), decreasing from about 800 to 650 s.

2.3. H₂O Effect on Cu Speciation

At this point, we used Gaussian deconvolution of the bimodal TPD profiles to compare the amount of NH₃ to Cu atoms and to Brønsted acid sites in wet and dry atmosphere. Notice that the NH₃ legated to the Al extra-framework was completely lost in the presence

of water, as apparent in Figure 3A for H-CHA (SAR 25) and in Figure S1 for H-CHA (SAR 13).

The results in Figure 5 and in Table S1 indicate that by cofeeding water: (i) the quantity of NH_3 stored on Brønsted sites slightly increased, while (ii) the Lewis NH_3 decreased. This trend could be related to the hydrolysis of $\text{Z}_2\text{Cu}^{\text{II}}$ species, reaction (6) [6,22]:

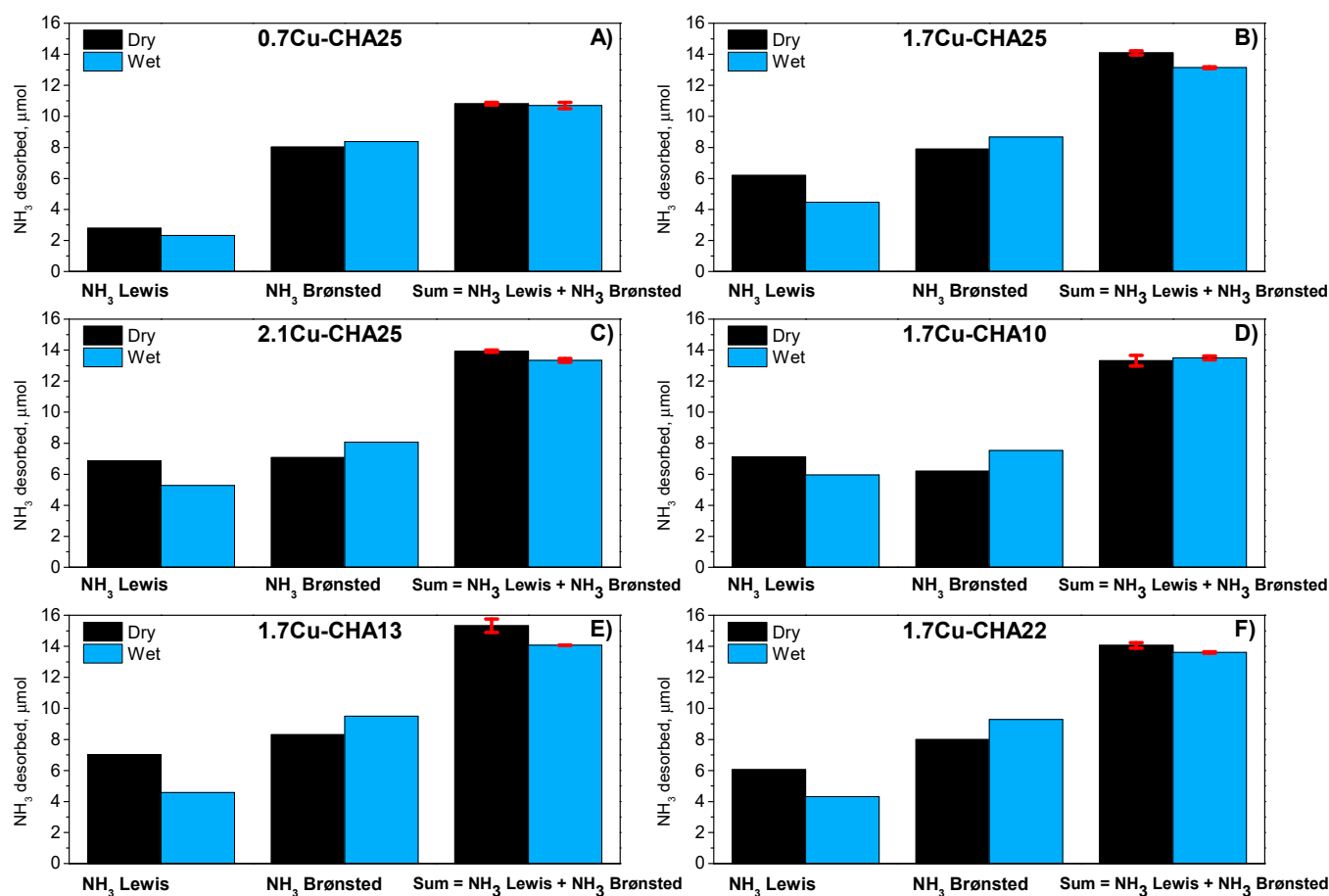
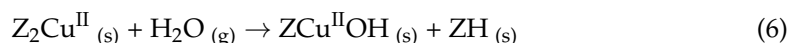


Figure 5. Deconvolution of the TPD profiles: evaluation of NH_3 stored on Lewis and Brønsted sites. Comparison between dry and wet conditions over different Cu-CHA samples: (A) 0.7% w/w Cu, SAR = 25; (B) 1.7% w/w Cu, SAR = 25; (C) 2.1% w/w Cu, SAR = 25; (D) 1.7% w/w Cu, SAR = 10; (E) 1.7% w/w Cu, SAR = 13; (F) 1.7% w/w Cu, SAR = 22. NH_3 = 500 ppm, H_2O = 0–5% v/v, He. GHSV = 266,250 $\text{cm}^3/(\text{g}_{\text{cat}}\cdot\text{h})$ (STP). Pre-oxidized catalysts. Red symbols = Error bar.

In fact, according to this reaction, the transformation of $\text{Z}_2\text{Cu}^{\text{II}}$ into $\text{ZCu}^{\text{II}}\text{OH}$ implies a loss in Cu- NH_3 ligands. Indeed, the $\text{Z}_2\text{Cu}^{\text{II}}$ species can bind up to four NH_3 molecules, while the hydroxylated Cu ions can coordinate only three molecules [5,8,23].

According to our deconvolution results, however, the increment in Brønsted NH_3 in wet conditions was less than the decrease in Lewis NH_3 for some samples. This behavior could be explained by a further loss of Lewis NH_3 due to the competitive adsorption of water on the Cu sites [20], as indicated by the decrease in the overall NH_3 storage capacity (i.e., the sum of Brønsted and Lewis NH_3 in Figure 5).

The fraction of $\text{Z}_2\text{Cu}^{\text{II}}$ transformed into $\text{ZCu}^{\text{II}}\text{OH}$ was estimated by the following equation:

$$\frac{\text{Amount of } \text{Z}_2\text{Cu}^{\text{II}} \text{ hydrolysed}}{\text{initial amount of } \text{Z}_2\text{Cu}^{\text{II}}(\text{Table 2})} = \frac{\text{NH}_3 \text{ Brønsted wet} - \text{NH}_3 \text{ Brønsted dry}}{\text{initial amount of } \text{Z}_2\text{Cu}^{\text{II}}(\text{Table 2})} \% \quad (7)$$

From the results in Table 2 it can be noticed that only a fraction of Z_2Cu^{II} (40–70%) was hydrolyzed after the wet NH_3 adsorption. Furthermore, even if 1.7Cu-SAR25 and 1.7Cu-SAR22 are characterized by similar speciation and Cu/Al ratio, they display different behaviors in a wet atmosphere, more specifically the 1.7Cu-SAR22 shows a more enhanced hydrolysis of the Z_2Cu^{II} sites. One possible parameter affecting this reaction could be the distribution of the Al atoms in the zeolite framework. In addition, two different types of the Z_2Cu^{II} sites are viable, with para and metal configuration, respectively, which show distinct features in EPR spectra and distinct reactivity under Standard SCR conditions [24]. In principle, these species could be associated with a different response to the hydrolysis reaction. A dedicated investigation of the hydrolysis reaction is ongoing.

Table 2. Estimates of the fraction of Z_2Cu^{II} hydrolyzed according to reaction (3).

Sample	Cu Loaded, μmol	Z_2Cu^{II} from NO_2 Adsorption, μmol [8]	NH_3 Brønsted dry, μmol	NH_3 Brønsted wet, μmol	Z_2Cu^{II} Hydrolysed/Initial Z_2Cu^{II} , %	Z_2Cu^{II} Hydrolysed/ Cu_{tot} , %
0.7% w/w Cu, SAR = 25	1.8	0.8	8.02	8.38	45	20
1.7% w/w Cu, SAR = 25	4.3	1.8	7.9	8.67	43	19
2.1% w/w Cu, SAR = 25	5.2	1.7	7.07	8.07	59	19
1.7% w/w Cu, SAR = 10	4.3	2.4	6.20	7.54	56	31
1.7% w/w Cu, SAR = 13	4.3	3.1	8.30	9.50	39	28
1.7% w/w Cu, SAR = 22	4.3	1.8	8.00	9.28	71	30

At this point we calculated the NH_3/Cu ratio, taking into account the area under the low-T TPD peak, proportional to the NH_3 stored only on Cu cations, and the number of copper atoms known from the weight fraction of Cu in each sample (Table 3). Figure 6 illustrates how this ratio varies with the Cu/Al ratio.

Table 3. Characterization of the tested catalyst samples [8].

Sample	Cu Loaded, μmol	Cu/Al Ratio, -	NO_2 Adsorption Experiment, μmol	$ZCu^{II}OH$, %	Z_2Cu^{II} , %	NO_x Conversion at 225 °C, %
0.7% w/w Cu, SAR = 25	1.8	0.11	1.0	55	45	16
1.7% w/w Cu, SAR = 25	4.3	0.24	2.5	58	42	91
2.1% w/w Cu, SAR = 25	5.2	0.29	3.5	67	33	96
1.7% w/w Cu, SAR = 10	4.3	0.12	1.9	44	56	58
1.7% w/w Cu, SAR = 13	4.3	0.17	1.2	28	72	67
1.7% w/w Cu, SAR = 22	4.3	0.22	2.5	58	41	83

Under dry conditions, the experimental data were in accordance with the literature [8,23]: the ratio was in the range 1–2 when only the Cu- NH_3 desorbed during the TPD was considered, and in the 3–4 range when the physisorbed NH_3 was also considered (area highlighted in orange, Figure 1A). In particular, the increase in Cu/Al lead to a decrease in the NH_3/Cu ratio, from a value close to 4 (or 2 considering only the TPD phase) for the catalysts with the lowest SAR and Cu loading, to a value closer to 3 (or 1 considering only the TPD phase) for the other tested samples (Figure 6). When water was added to the system, we observed a shift of all the NH_3/Cu ratios evaluated from the TPD to values

closer to 3 (or 1 considering only the TPD phase). These results are consistent both with competition between H₂O and NH₃ adsorption onto Lewis sites and with the hydrolysis of a fraction of Z₂Cu^{II} species into ZCu^{II}OH according to reaction (6), as discussed above.

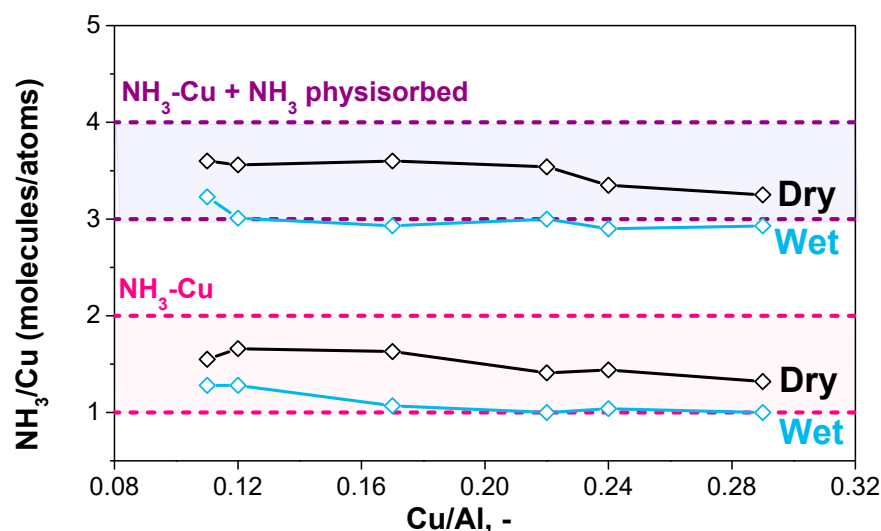


Figure 6. NH₃/Cu ratio evaluated considering only NH₃ stored on Cu ions (low-T peak of TPD) and NH₃ stored on Cu ions plus NH₃ physisorbed: comparison between dry and wet conditions.

At this stage of the discussion, our opinion is that analysis of the NH₃-TPD data is not the best method to probe the Cu speciation. First, quantification of the Lewis and Brønsted acid sites requires deconvolution of the NH₃-TPD curves. Second, during the temperature ramp the Cu atoms are reduced, producing N₂; hence, it would be important to include its trace in the TPD plot to accurately analyze the experimental data. Finally, under wet conditions the Cu species are modified by the hydrolysis reaction. The occurrence of these phenomena complicates the interpretation of experimental TPD traces, thus it is suggested not to solely use this method to quantify the fraction of Z₂Cu^{II} and ZCu^{II}OH species in the catalysts. The Cu speciation could be quantified by means of simpler techniques such as, for example, NO₂ adsorption + TPD and H₂ TPR, as discussed in [8,11,25]. However, NH₃-TPD runs under wet conditions provide useful experimental evidence of the hydrolysis reaction over Cu-CHA materials.

3. Material and Methods

For this study, we investigated two sets of Cu-exchanged chabazite (Cu-CHA), research catalysts supplied in the form of powders by Johnson Matthey. One set was purposely characterized by different SiO₂/Al₂O₃ (SAR) ratios (10, 13, 22, 25), with fixed Cu loading = 1.7% *w/w*. The other had different Cu loadings (0, 0.7, 1.7, 2.1% *w/w*, with fixed SAR = 25). The textural properties of some samples, comprising the BET surface area and the micropore volume, are reported in Table S3 and are typical of commercial CHA based materials [26,27]. The samples were conditioned by heating them up to 600 °C at 5 °C/min and holding the maximum temperature for 5 h, while 10% O₂ and 10% H₂O were fed in to remove all the impurities and the species that may be formed on the sample due to contact with atmosphere.

Sixteen milligrams of catalyst powder, sieved to obtain an average particle size of 90 micron and diluted up to 130 mg with cordierite, was loaded into a quartz flow reactor (6 mm ID) inserted in a vertical electric furnace. The temperature was controlled by a K-type thermocouple directly immersed in the catalyst bed.

Helium was used as balance gas in all the micro-reactor runs. Gases were controlled using mass flow controllers (Brooks Instruments, Hatfield, PA, USA). Water vapor was fed in by means of a saturator and the water concentration was controlled by adjusting the saturator's temperature according to Antoine's Law. NH₃ was fed in using a 6-way valve,

enabling step changes in the reactant concentrations. Temporal evolution of the species at the reactor outlet was followed by a mass spectrometer (QGA Hiden Analytical, Warrington, UK) and a UV analyzer (ABB LIMAS 11 HW, Zurich, Switzerland) arranged in a parallel configuration, which allowed the simultaneous measurement of all the species involved.

The interaction between NH_3 molecules and the catalyst was studied by performing NH_3 adsorption + temperature programmed desorption (TPD) runs. The catalysts were saturated using 500 ppm of NH_3 and balance He (GHSV = $266,250 \text{ cm}^3/(\text{g}_{\text{cat}} \cdot \text{h})$ STP), both under dry and wet conditions (5% *w/w* H_2O), at $150 \text{ }^\circ\text{C}$. After that, the catalysts were purged with He (or He + H_2O) for 1 h to desorb weakly bound ammonia, and then heated in He only (or He + H_2O) from $150 \text{ }^\circ\text{C}$ up to $550 \text{ }^\circ\text{C}$ at a rate of $15 \text{ }^\circ\text{C}/\text{min}$ to release the strongly adsorbed molecules. Prior to each experiment, in order to control the oxidation state of the catalysts, the samples were pre-treated at $550 \text{ }^\circ\text{C}$, feeding 8% O_2 in He for 1 h, then the adsorption temperature was reached by cooling down under the same gas feed, with a final purge in He for 15 min.

The catalysts were characterized in our previous work [8], the amount of Cu loaded and the Cu speciation is reported in Table 3. In particular, $\text{NO} + \text{NH}_3$ TPR and ICP-MS analysis were used to quantify the number of reducible Cu^{II} sites. Meanwhile, the NO_2 adsorption-TPD protocol was implemented to assess the amount of $\text{ZCu}^{\text{II}}\text{OH}$ species [8]. The samples show the typical de NO_x activity of CHA based materials as apparent from the NO conversions in Standard SCR conditions reported in Table 3 (i.e., GHSV = $937,500 \text{ cm}^3/\text{h}/\text{g}_{\text{cat}}$ (STP), $\text{g}_{\text{cat}} = 0.016 \text{ g}$, $\text{NH}_3 = 500 \text{ ppm}$, $\text{NO} = 500 \text{ ppm}$, $\text{H}_2\text{O} = 5\%$, $\text{O}_2 = 8\%$, $T = 225 \text{ }^\circ\text{C}$).

4. Conclusions

Herein, we have studied the effect of H_2O on the NH_3 storage onto different Cu-CHA catalysts, using standard NH_3 adsorption/TPD experiments. According to our preliminary results, during the temperature ramp of the TPD run the adsorbed NH_3 fully reduces the initially oxidized Cu sites, releasing a stoichiometric amount of N_2 . This effect is often overlooked in the literature but impacts the quantification of Cu-related and Brønsted NH_3 adsorption sites.

On increasing both the SAR and Cu loading, we found the adsorbed NH_3/Cu ratio decreased from 4 to 3 when H_2O was absent from the gas mixture (and from 2 to 1 in the absence of gaseous NH_3), which correlates nicely with the corresponding expected increase in the proportion of $\text{ZCu}^{\text{II}}\text{OH}$ over $\text{Z}_2\text{Cu}^{\text{II}}$ species. Upon addition of water to the feed stream, all the tested catalysts showed NH_3/Cu ratios closer to 3 (or to 1 in the absence of gaseous NH_3). These results are consistent both with the hydrolysis of a fraction of $\text{Z}_2\text{Cu}^{\text{II}}$ species to form $\text{ZCu}^{\text{II}}\text{OH}$, even though competition between H_2O and NH_3 for adsorption onto Lewis sites cannot be ruled out.

This work is novel because it includes both the Cu reduction and the hydrolysis reaction in the analysis of the NH_3 -TPD data. However, the occurrence of these phenomena complicates the interpretation of the experimental TPD runs, thus it is suggested not to solely use this method to probe the Cu speciation in Cu-CHA catalysts [8].

Supplementary Materials: The following are available online at <https://www.mdpi.com/article/10.3390/catal11070759/s1>, Figure S1: Comparison between dry and wet NH_3 -TPD after adsorption at $150 \text{ }^\circ\text{C}$ on H-CHA catalysts with SAR = 13, Table S1: NH_3 adsorbed on different sites as estimated from NH_3 -TPD deconvolution under dry conditions, Table S2: NH_3 adsorbed on different sites as estimated from NH_3 -TPD deconvolution under dry conditions.

Author Contributions: Conceptualization, J.C., A.P.E.Y. and D.T.; Data curation, R.V., F.G. and U.I.; Investigation, R.V.; Supervision, I.N. and E.T.; Visualization, S.L., J.C., A.P.E.Y. and D.T.; Writing—original draft, R.V.; Writing—review & editing, F.G., U.I. and M.P.R. All authors have read and agreed to the published version of the manuscript.

Funding: This research received no external funding.

Institutional Review Board Statement: Not applicable.

Informed Consent Statement: Not applicable.

Conflicts of Interest: The authors declare no conflict of interest.

References

1. Güthenke, A.; Chatterjee, D.; Weibel, M.; Krutzsch, B.; Kočí, P.; Marek, M.; Nova, I.; Tronconi, E. Current status of modeling lean exhaust gas aftertreatment catalysts. *Adv. Chem. Eng.* **2007**, *33*, 103–283. [[CrossRef](#)]
2. Nova, I.; Tronconi, E. *Urea-SCR Technology for deNO_x After Treatment of Diesel Exhausts*; Springer: New York, NY, USA, 2014.
3. Wang, D.; Zhang, L.; Li, J.; Kamasamudram, K.; Epling, W.S. NH₃-SCR over Cu/SAPO-34-Zeolite acidity and Cu structure changes as a function of Cu loading. *Catal. Today* **2014**, *231*, 64–74. [[CrossRef](#)]
4. Luo, J.; Gao, F.; Kamasamudram, K.; Currier, N.; Peden, C.H.F.; Yezerets, A. New insights into Cu/SSZ-13 SCR catalyst acidity. Part I: Nature of acidic sites probed by NH₃ titration. *J. Catal.* **2017**, *348*, 291–299. [[CrossRef](#)]
5. Paolucci, C.; Parekh, A.A.; Khurana, I.; Di Iorio, J.R.; Li, H.; Albarracin Caballero, J.D.; Shih, A.J.; Anggara, T.; Delgass, W.N.; Miller, J.T.; et al. Catalysis in a cage: Condition-dependent speciation and dynamics of exchanged Cu cations in SSZ-13 zeolites. *J. Am. Chem. Soc.* **2016**, *138*, 6028–6048. [[CrossRef](#)] [[PubMed](#)]
6. Gao, F.; Peden, C.H.F. Recent progress in atomic-level understanding of Cu/SSZ-13 selective catalytic reduction catalysts. *Catalysts* **2018**, *8*, 140. [[CrossRef](#)]
7. Rizzotto, V.; Chen, D.; Tabak, B.M.; Yang, J.Y.; Ye, D.; Simon, U.; Chen, P. Spectroscopic identification and catalytic relevance of NH₄⁺ intermediates in selective NO_x reduction over Cu-SSZ-13 zeolites. *Chemosphere* **2020**, *250*, 126272. [[CrossRef](#)] [[PubMed](#)]
8. Villamaina, R.; Liu, S.; Nova, I.; Tronconi, E.; Ruggeri, M.P.; Collier, J.; York, A.; Thompsett, D. Speciation of Cu Cations in Cu-CHA Catalysts for NH₃-SCR: Effects of SiO₂/AlO₃ Ratio and Cu-Loading Investigated by Transient Response Methods. *ACS Catal.* **2019**, *9*, 8916–8927. [[CrossRef](#)]
9. Song, J.; Wang, Y.; Walter, E.D.; Washton, N.M.; Mei, D.; Kovarik, L.; Engelhard, M.H.; Proding, S.; Wang, Y.; Peden, C.H.F.; et al. Toward Rational Design of Cu/SSZ-13 Selective Catalytic Reduction Catalysts: Implications from Atomic-Level Understanding of Hydrothermal Stability. *ACS Catal.* **2017**, *7*, 8214–8227. [[CrossRef](#)]
10. Fan, C.; Chen, Z.; Pang, L.; Ming, S.; Zhang, X.; Albert, K.B.; Liu, P.; Chen, H.; Li, T. The influence of Si/Al ratio on the catalytic property and hydrothermal stability of Cu-SSZ-13 catalysts for NH₃-SCR. *Appl. Catal. A Gen.* **2018**, *550*, 256–265. [[CrossRef](#)]
11. Gao, F.; Washton, N.M.; Wang, Y.; Kollár, M.; Szanyi, J.; Peden, C.H.F. Effects of Si/Al ratio on Cu/SSZ-13 NH₃-SCR catalysts: Implications for the active Cu species and the roles of Brønsted acidity. *J. Catal.* **2015**, *331*, 25–38. [[CrossRef](#)]
12. Daya, R.; Joshi, S.Y.; Luo, J.; Dadi, R.K.; Currier, N.W.; Yezerets, A. On kinetic modeling of change in active sites upon hydrothermal aging of Cu-SSZ-13. *Appl. Catal. B Environ.* **2020**, *263*, 118368. [[CrossRef](#)]
13. Borfecchia, E.; Negri, C.; Lomachenko, K.A.; Lamberti, C.; Janssens, T.V.W.; Berlier, G. Temperature-dependent dynamics of NH₃-derived Cu species in the Cu-CHA SCR catalyst. *React. Chem. Eng.* **2019**, *4*, 1067–1080. [[CrossRef](#)]
14. Giordanino, F.; Borfecchia, E.; Lomachenko, K.A.; Lazzarini, A.; Agostini, G.; Gallo, E.; Soldatov, A.V.; Beato, P.; Bordiga, S.; Lamberti, C. Interaction of NH₃ with Cu-SSZ-13 catalyst: A complementary FTIR, XANES, and XES study. *J. Phys. Chem. Lett.* **2014**, *5*, 1552–1559. [[CrossRef](#)]
15. Ruggeri, M.P.; Nova, I.; Tronconi, E.; Collier, J.E.; York, A.P.E. Structure–Activity Relationship of Different Cu–Zeolite Catalysts for NH₃-SCR. *Top. Catal.* **2016**, *59*, 875–881. [[CrossRef](#)]
16. Hu, W.; Selleri, T.; Gramigni, F.; Fenes, E.; Rout, K.R.; Liu, S.; Nova, I.; Chen, D.; Gao, X.; Tronconi, E. On the Redox Mechanism of Low-Temperature NH₃-SCR over Cu-CHA: A Combined Experimental and Theoretical Study of the Reduction Half Cycle. *Angew. Chem.* **2021**, *133*, 7273–7280. [[CrossRef](#)]
17. Gao, F.; Wang, Y.; Washton, N.M.; Kollár, M.; Szanyi, J.; Peden, C.H.F. Effects of Alkali and Alkaline Earth Cations on the Activity and Hydrothermal Stability of Cu/SSZ-13 NH₃-SCR Catalysts. *ACS Catal.* **2015**, *5*, 6780–6791. [[CrossRef](#)]
18. Han, S.; Ye, Q.; Cheng, S.; Kang, T.; Dai, H. Effect of the hydrothermal aging temperature and Cu/Al ratio on the hydrothermal stability of CuSSZ-13 catalysts for NH₃-SCR. *Catal. Sci. Technol.* **2017**, *7*, 703–717. [[CrossRef](#)]
19. Bagnasco, G. Improving the selectivity of NH₃ TPD measurements. *J. Catal.* **1996**, *159*, 249–252. [[CrossRef](#)]
20. Sjøvall, H.; Blint, R.J.; Olsson, L. Detailed Kinetic Modeling of NH₃ and H₂O Adsorption, and NH₃ Oxidation over Cu-ZSM-5. *J. Phys. Chem. C* **2009**, *113*, 1393–1405. [[CrossRef](#)]
21. Bolis, V.; Busco, C.; Ugliengo, P. Thermodynamic study of water adsorption in high-silica zeolites. *J. Phys. Chem. B* **2006**, *110*, 14849–14859. [[CrossRef](#)] [[PubMed](#)]
22. Gao, F.; Mei, D.; Wang, Y.; Szanyi, J.; Peden, C.H.F. Selective Catalytic Reduction over Cu/SSZ-13: Linking Homo- and Heterogeneous Catalysis. *J. Am. Chem. Soc.* **2017**, *139*, 4935–4942. [[CrossRef](#)] [[PubMed](#)]
23. Paolucci, C.; Khurana, I.; Parekh, A.A.; Li, S.; Shih, A.J.; Li, H.; Di Iorio, J.R.; Albarracin-Caballero, J.D.; Yezerets, A.; Miller, J.T.; et al. Dynamic multinuclear sites formed by mobilized copper ions in NO_x selective catalytic reduction. *Science* **2017**, *357*, 898–903. [[CrossRef](#)]
24. Godiksen, A.; Isaksen, O.L.; Rasmussen, S.B.; Vennestrøm, P.N.R.; Mossin, S. Site-Specific Reactivity of Copper Chabazite Zeolites with Nitric Oxide, Ammonia, and Oxygen. *ChemCatChem* **2018**, *10*, 366–370. [[CrossRef](#)]
25. Hun Kwak, J.; Zhu, H.; Lee, J.H.; Peden, C.H.F.; Szanyi, J. Two different cationic positions in Cu-SSZ-13? *Chem. Commun.* **2012**, *48*, 4758–4760. [[CrossRef](#)] [[PubMed](#)]

-
26. Rutkowska, M.; Duda, M.; Kowalczyk, A.; Chmielarz, L. Modification de la zéolithe CHA commerciale pour les besoins de la réduction catalytique des oxydes d'azote. *C. R. Chim.* **2017**, *20*, 850–859. [[CrossRef](#)]
 27. McEwen, J.S.; Anggara, T.; Schneider, W.F.; Kispersky, V.F.; Miller, J.T.; Delgass, W.N.; Ribeiro, F.H. Integrated operando X-ray absorption and DFT characterization of Cu-SSZ-13 exchange sites during the selective catalytic reduction of NO_x with NH₃. *Catal. Today* **2012**, *184*, 129–144. [[CrossRef](#)]